THE UNIVERSITY of EDINBURGH

Edinburgh Research Explorer

# Transcription factor, Wilms' Tumour 1 regulates developmental RNAs through 3' UTR interaction.

**Citation for published version:**
Bharathavikru, R, Dudnakova, T, Aitken, J, Slight, J, Artibani, M, Hohenstein, P, Tollervey, D & Hastie, N 2017, 'Transcription factor, Wilms' Tumour 1 regulates developmental RNAs through 3' UTR interaction.' Genes & Development, vol. 31, no. 4, pp. 347-352. DOI: 10.1101/gad.291500.116

**Digital Object Identifier (DOI):**
10.1101/gad.291500.116

**Link:**
Link to publication record in Edinburgh Research Explorer

**Document Version:**
Publisher's PDF, also known as Version of record

**Published In:**
Genes & Development

**Publisher Rights Statement:**
Creative Commons License (Attribution 4.0 International), as described at http://creativecommons.org/licenses/by/4.0

**General rights**
Copyright for the publications made accessible via the Edinburgh Research Explorer is retained by the author(s) and / or other copyright owners and it is a condition of accessing these publications that users recognise and abide by the legal requirements associated with these rights.

**Take down policy**
The University of Edinburgh has made every reasonable effort to ensure that Edinburgh Research Explorer content complies with UK legislation. If you believe that the public display of this file breaches copyright please contact openaccess@ed.ac.uk providing details, and we will remove access to the work immediately and investigate your claim.

OPEN ACCESS

Download date: 05. Apr. 2019

# Transcription factor, Wilms' Tumour 1 regulates developmental RNAs through 3' UTR interaction.

Ruthrothaselvi Bharathavikru[1,4], Tatiana Dudnakova[2,4], Stuart Aitken[1], Joan Slight[1], Mara Artibani[1,5], Peter Hohenstein[1,3], David Tollervey[2], Nick Hastie[1*]

[1]MRC Institute of Genetics and Molecular Medicine, University of Edinburgh, Western General Hospital, Crewe Road (S), Edinburgh, EH4 2XU, [2]Wellcome Trust Centre for Cell Biology, Kings Buildings, University of Edinburgh, EH9 3BF, [3]Roslin Institute, The University of Edinburgh, Easter Bush, Midlothian, EH25 9RG

4-equal contribution

5-present address: Weatherall Institute of Molecular Medicine, University of Oxford

*Corresponding author, Email for correspondence: nick.hastie@igmm.ed.ac.uk

**Abstract:**

Wilms' tumour 1 (WT1) is essential for development and homeostasis of multiple mesodermal tissues. Despite evidence for post transcriptional roles, no endogenous WT1 target RNAs exist. Using RNA immunoprecipitation and UV-crosslinking, we show WT1 binds preferentially to 3' UTRs of developmental targets. These target mRNAs are downregulated upon WT1 depletion in cell culture and developing kidney mesenchyme. *Wt1* deletion leads to rapid turnover of specific mRNAs. WT1 regulates reporter gene expression through interaction with 3' UTR binding sites. Combining, experimental and computational analyses, we propose that WT1 influences key developmental and disease processes in part through regulating mRNA turnover.

**KEYWORDS:** WT1, FLASH, 3' UTR, Hybrids, RNA secondary structures, Developmental pathways

**Running Title:** WT1 interacts with 3'UTR of developmental targets

## Introduction

The different steps in gene expression, from transcription through a series of post transcriptional events, are closely interconnected and some multifunctional proteins regulate several points in this pathway. One potential example is the Wilms' tumour gene, *WT1*. Mice

lacking *Wt1* die at mid-gestation, through defective coronary vasculature, suffer from congenital diaphragmatic hernia, have no kidneys, gonads, spleen or adrenals. All these defects can be traced to a key role for WT1 in the development of tissues derived from the intermediate and lateral plate mesoderm. In humans, germ line *WT1* mutations lead to the eponymous pediatric cancer, genitourinary anomalies and in some cases congenital diaphragmatic hernia and heart disease (**Chau and Hastie 2012**).

Furthermore, WT1 is a key regulator of the balance between mesenchymal and epithelial states in these tissues, being required for the mesenchyme to epithelial transition (MET), a key step in nephron formation, and for the epithelial to mesenchyme transition (EMT) that produces coronary vascular progenitors from the epicardium. WT1 also plays essential roles in adult tissue homeostasis. Hence ubiquitous deletion of *Wt1* in adult mice leads to acute kidney glomerulosclerosis, atrophy of the exocrine pancreas and spleen and widespread reduction in bone and fat (**Chau et al. 2011**). A recent study showed that WT1 is reactivated during tissue repair and during adult tumorigenesis where it is required in the mesenchymal component and vasculature for tumour growth (**Wagner et al. 2014**).

The molecular mechanisms by which WT1 fulfils these apparently diverse roles have been attributed to its transcriptional function. Accordingly, there is substantial evidence that WT1 binds genomic DNA and regulates transcription, acting either as an activator or repressor (**Essafi et al. 2011; Toska and Roberts 2014**). A growing number of physiological WT1 transcriptional targets have been identified in development, homeostasis and disease (**Motamedi et al. 2014; Kann et al. 2015; Dong et al. 2015**). However, the evidence suggests that transcriptional regulation is not the only WT1 function.

The two major essential isoforms (**Barbaux et al. 1997**; **Hammes et al. 2001**) conserved throughout vertebrate evolution are created by an alternative splice that inserts three amino acids (lysine-threonine-serine; KTS) between the third and fourth zinc finger (**Hastie 2001**). The first suggestion that WT1 may function post-transcriptionally came from **Larsson et al. 1995,** showing that the + KTS isoforms associate with splicing factors. WT1 was then shown to integrate into active splice complexes by interacting with the splicing factor U2AF65 (**Davies et al. 1998**). Moreover, WT1 binds both RNA and DNA with similar binding efficiencies as demonstrated by structural and kinetic studies (**Bardeesy and Pelletier 1998; Caricasole et al. 1996; Zhai et al. 2001**). Structural modelling studies also identified an RNA recognition motif (RRM) in WT1 **(Kennedy et al. 1996).** Further support for posttranscriptional roles for WT1 was provided by **Niksic et al. 2004,** showing that all isoforms shuttle between nucleus and cytoplasm where they are located on actively

translating ribosomes. In particular, the +KTS isoforms were shown to recruit transcripts containing a viral RNA sequence to polysomes, regulating their translation (**Bor et al. 2006**). A considerable amount of data therefore supports roles for WT1 from splicing through to translation. However, causal evidence for direct WT1 functions in specific steps, and understanding of the mechanisms involved, have been limited by the absence of characterized endogenous WT1 RNA targets. To address this, we identified WT1 interacting RNAs in mouse ES cells and a mesonephric cell line by a combination of RNA-immunoprecipitation and sequencing (RIP-seq) and a modification of the CLASH UV-crosslinking technique (**Helwak et al. 2013**) termed FLASH. The latter identifies RNAs that directly interact with WT1 as well as RNA-RNA duplexes formed by these target RNAs. The interaction of intramolecular RNA hybrids is increased in the presence of WT1. This study provides strong evidence that the tumour suppressor protein, WT1 regulates physiologically important RNAs and their stability through interactions with 3' untranslated regions (3' UTRs).

## Results and Discussion:

### WT1 binds to multiple categories of RNA

RNA IP (RIP, **Bharathavikru and Dudnakova 2016**) was performed on ES cells and mesonephric M15 cells along with negative control RIP to identify RNAs that interact with endogenous WT1. The specificity of the antibody was verified by immuno- pulldown and western blotting (**Supplemental Fig. S1A).** Recovered RNAs were identified by RT PCR and Illumina sequencing. Overall numbers of reads obtained are presented in **Supplemental Fig. S1B**. Reads were mapped to the mouse genome and analyzed for different RNA categories (**Fig. 1A**). RIP data were processed to identify regions where the number of uniquely aligned reads passed statistical significance (FDR<0.05; minimum of 5 reads), and overlapping regions of aligned reads were clustered (minimum of 5 reads) using the pyCRAC software (**Webb et al. 2014**). The RNA biotypes of these clusters were determined using Ensembl annotations. Strikingly, WT1 targets were predominantly (96%) identified as protein coding mRNAs (**Fig. 1A**). Amongst ncRNA targets, the majority were long intergenic noncoding (linc) RNAs followed by microRNAs (miRNAs) and small nucleolar RNAs (snoRNAs). Closer examination of the position on protein-coding genes of significant clusters revealed higher recovery of sequences at the 5' and 3' end of transcripts and the UTRs (**Fig. 1B**). A number of transcripts had notably high read coverage including those for *Igfbp5*, shown as an example in **Fig. 1C.**

To confirm the sequence data, RIP reactions were performed followed by PCR across different regions of selected protein-coding transcripts (**Fig. 1D** and **Supplemental Fig. S1C**). For most of the selected targets including *Igfbp5* the results were in good agreement with the RIP-seq analysis, showing significant enrichment towards the 3' UTR. In order to assess the functional relevance of the WT1 interacting RNA, a gene ontology analysis was performed. Several developmental pathways that are regulated by WT1 were identified as significant GO categories in this analysis, including coronary vasculature development and wnt signaling pathway (**Supplemental Fig. S1D and S1E, Supplemental Tables S1 and S2).**

**UV crosslinking confirms WT1 enrichment over the 3' UTR of mRNAs**

To identify specific protein-RNA interaction sites, we adopted a UV cross-linking approach. Since ncRNAs were identified among WT1 interacting RNA (**Fig. 1A**), we applied an experimental strategy that can identify RNA-RNA interactions. The crosslinking and sequencing of hybrids (CLASH) technique can identify both RNA-protein and RNA-RNA interactions, but requires the use of epitope-tagged "bait" proteins (**Helwak et al. 2013**). We developed a modified technique, formaldehyde-assisted crosslinking and sequencing of hybrids (FLASH) (**Fig. 2A**). This allowed the antibody-based IP of endogenous WT1 and recovery of crosslinked RNAs in the M15 cell line.

Reads obtained from FLASH experiments were analyzed separately for protein-RNA interactions and for protein associated RNA-RNA hybrids (**Webb et al. 2014; Travis et al. 2014**). The assignment of significant clusters to biotypes showed that the major category of interacting RNA was protein coding transcripts (**Fig. 2B**), consistent with the RIP-seq data. The most enriched ncRNAs. were snoRNAs (different from RIP-seq due to the difference in methodology), followed by similar numbers of miRNAs and lincRNAs. On mRNAs, WT1 binding sites showed strong enrichment over the 3' end of the ORFs and 3' UTRs (**Fig. 2C**), in comparison to input and control IgG FLASH (**Supplemental Fig. S2**). GO analysis of the terms associated with the WT1 interacting RNAs (**Supplemental Table S3)** showed enrichment for developmental pathways, cell adhesion and cell migration, similar to the RIP-seq data. A gene ontology chart generated by REVIGO is shown in **Fig. 2D**. Thus, WT1 was found to interact with developmental regulators, as identified by both RIP-seq and FLASH.

**WT1 associates with RNA at the 3' UTR through secondary structures**

The FLASH analysis includes ligation steps that can lead to the formation of hybrid cDNAs derived from two independent RNA molecules (intermolecular), or from non-contiguous

sequences of the same RNA (intramolecular/gene-self). To investigate whether WT1 interacts with secondary structured RNA or other RNA duplexes, we analyzed the WT1 FLASH data for chimeric reads derived from RNA hybrids using the hyb software pipeline (**Travis et al. 2014**). In the FLASH data, 0.49% of reads were identified as hybrids, consistent with recovery in previous analyses. The control input data for the WT1 RIP was similarly analyzed which showed 0.03% hybrids.

A representation of the different hybrids obtained in WT1 FLASH is shown in **Fig. 3A**. The different datasets of WT1 interacting RNA show a reasonable overlap (60% of the protein-coding genes identified by FLASH were also found by RIP-Seq; **Supplemental Table S4).** Interactions recovered within 3' UTR sequences were most frequently intramolecular, comprising 52% of hybrids. Intermolecular interactions between mRNAs and microRNAs (miRNAs) were ~10-fold less frequent, comprising 5% of hybrids with 964 unique interactions. Notably, in human AGO1 data mRNA-miRNA interactions were 3-fold more numerous than intramolecular interactions within 3' UTRs (**Helwak et al. 2013**). In addition, the mean energy of intermolecular 3'UTR base-pairing was -15.1 kcal/mol in the FLASH data, significantly less than in the control -7.3 kcal/mol ($p<2.2e-16$ by Wilcoxon rank sum test) (**Fig. 3A, Supplemental Fig. S3A and S3B**). Several interactions were between non-contiguous sequences that were sufficiently close to allow folding prediction for the RNA to assess their stability. Representative examples of local contacts (**Fig. 3B**) and those with extended secondary structures are shown in **Fig. 3C**. These structures have lower hybridization energy indicating a more stable structure.

During the preparation of this manuscript, RNA-RNA interactions using psoralen crosslinking were identified. We compared the RNA hybrids identified by Psoralen Analysis of RNA Interactions (PARIS) (**Lu et al. 2016**) to the RNA hybrids identified by WT1 FLASH. Analysis of WT1 interacting *Podxl, Igfbp3, Upk3b, Ctdsp2*, revealed a difference in the location and energy of the hybrids and the strength of the hybrids (**Fig. 3D, Supplemental Fig. S3C**). Thus, in the presence of WT1 there is an increase in the number of stable intramolecular RNA interactions, supporting a role for WT1 as a nucleating centre for these interactions. Recent studies with the double-stranded RNA binding protein, Staufen (**Sugimoto et al. 2015**) show secondary RNA structures to be common and functionally important for gene expression. WT1 interaction at the 3' UTR of targets also show secondary structures suggesting a role in regulating RNA stability. To assess the potential of the predicted, WT1-bound, RNA structures, we analyzed the hybrid sequences for the presence of any miRNA binding sites. A significant

proportion of hybrids were found to harbor clusters of miRNA binding sites (**Supplemental Fig. S3D, Supplemental Table S5**).

Since its identification as an RNA binding protein, it has been speculated that WT1 associated RNA binding may not be exclusively determined by sequence. This was indeed shown with WT1 Zinc fingers (Zf) and RNA aptamers cloned based on the SELEX motifs, which showed that WT1 Zf-RNA interaction was not just sequence dependent but also required a hairpin loop structure adjacent to the consensus motif (**Zhai et al. 2001**).This is in agreement with our hybrids analysis, which shows that WT1 interacts with stable RNA secondary structures. The exact contribution of sequence and structural requirements for the interaction require further investigation.

**WT1 regulates the expression of a subset of the RNA binding targets**

As the WT1 RNA interaction data support a role in RNA stability, we assessed whether the expression levels of these targets were also regulated by WT1. The results by cuffdiff analysis (**Trapnell et al. 2012**) are summarized in **Fig. 4A**. Of the differentially expressed genes in ES cells on *Wt1* KO (using an adjusted p value of 0.05 and with fragments per kilobase of transcript per million mapped reads (FPKM) ≥1 in at least one condition), 92 genes were upregulated and 67 downregulated. In M15, 156 genes were differentially expressed on *Wt1* knockdown (also see **Supplemental Fig. S4**), with 50 genes upregulated and 106 downregulated.

In M15 cells, 40% and 26% of differentially regulated genes were identified by RIP-seq and FLASH respectively. In ES cells, 26% of differentially regulated genes were identified as interacting with WT1 by RIP-seq. 45 of the differentially regulated genes in M15 cells, were found to have 267 gene- self hybrids from the FLASH analysis. Importantly, 252 of these hybrids were associated with downregulated genes and very few of the WT1 interacting RNAs (6%) were upregulated. GO enrichment analysis of genes differentially regulated in both ES and M15 cells upon downregulation of *Wt1* showed enrichment for pathways such as cell adhesion, positive regulation of developmental processes, wnt signaling, cell proliferation, skeletal system development and urogenital system development (**Fig. 4B, Supplemental Tables S6 and S7**). These processes are all disrupted through *Wt1* mutation or loss but the mechanistic details have remained incomplete (**Chau and Hastie 2012**).

The expression changes found in the RNA-seq data were validated by qRT-PCR in both ES cells and M15 cells for representative genes, associated with the most significant GO terms.

This analysis confirmed the downregulation of the following RNA binding targets with significant *p* values. These include *Rspo1* and *Wnt2b* for wnt signalling; *Cdh11* and *Podxl* for adhesion, *Igfbps* for IGF signalling and *Gas1* for proliferation. Other targets that followed similar trend in both RNA-seq and qRT PCR include *Wnt2b* and the mesothelial marker *Upk3b*. WT1 has recently been shown to regulate a subset of mesothelial origin progenitors towards the fat lineage (**Chau et al. 2014**). Selected upregulated candidate genes including *Mt2* and *Hnf1b* were also validated by qRT-PCR (**Fig. 4C**).

In order to validate the findings in embryonic tissue, expression of selected target genes (*Rspo1, Cdh11, Podxl and Gas1*) was compared in FACS sorted wildtype versus *Wt1* mutant metanephric mesenchyme from E13.5 kidney cells. These were obtained by crossing the *Nes-Cre* and *Wt1*co alleles with a *Wt1GFP* knock-in model (**Essafi et al. 2011**). GFP+ cells from GFP control ($Wt1^{co/GFP}$), GFP- cells from cre control ($Nes\text{-}Cre^{Wt1co/+}$) and *Wt1*-deficient ($Nes\text{-}Cre\ Wt1^{co/GFP}$) were compared for expression. qRT-PCR analysis of the selected candidates showed up to 30 fold downregulation of expression in the absence of *Wt1* (**Fig. 4D**), confirming the physiological relevance of these observations.

**The majority of WT1 dependent-RNA binding targets are not WT1 Transcriptional Targets**

WT1 is known to both activate and repress transcription (reviewed in **Toska and Roberts 2014)**. In contrast, the global RNA interactome analysis supports a role for WT1 as an RNA binding protein, functioning by interacting with the 3' UTR of RNA and potentially regulating stability. Here, we have shown that a significant number of the WT1 interacting RNA targets are reduced upon *Wt1* deletion/knockdown, reflecting WT1-mediated upregulation at transcriptional and/or post transcriptional steps.

Consistent with post transcriptional effects of WT1, a correlation was observed between the ratios of coverage (proportion of the length of the 3' UTR with reads mapped) and RPKM between RNA interaction and transcriptome changes (**Fig. 5A and Supplemental Fig. S5A**). Downregulated genes in ES have increased WT1 coverage and Reads per kilobase per million mapped reads (RPKM) ratios in comparison to unregulated genes ($p < 2.2e\text{-}16$ by Wilcoxon rank sum test) or upregulated genes ($p < 8.2e\text{-}14$ by Wilcoxon rank sum test). Similarly, recurrent kmers occurring in 3' UTRs were identified in the single read FLASH data. The polyadenylation signal AATAAA had the highest Z score, and three similar sequences were also found in the top 10 kmers. However, on correlation with downregulation, TGTAAAT

motif was found by MEME (**Bailey and Elkan, 1994**) at 294 sites (e value $2.7^{e-562}$), which is different from the motif identified by RIP-seq (**Supplemental Fig. S5B, S5C**).
To investigate whether downregulated, WT1 target mRNAs are also directly regulated by transcription, we compared them to published WT1 ChIP-seq data (**Motamedi et al. 2014).** On comparing the 156 differentially regulated genes from the M15 transcriptome analysis, to the published set of 1771 WT1 ChIPseq targets, there were 22 overlapping targets. Of the 38 most downregulated and interacting RNA targets identified in our study, only 7 were present in the above transcriptional target dataset (**Supplemental Table S8**). A summary of the overlap between the RNA interacting candidates, differentially regulated targets and ChIP-seq targets identified by the different analyses in relation to the transcriptome analysis is presented in **Supplemental Fig. S5D**.

**WT1 regulates RNA stability**

To test whether, as hypothesized, WT1 regulates the turnover of target RNAs, wildtype and *Wt1* depleted cells were treated with actinomycin and RNA decay was measured using qPCR. As shown in **Fig. 5B**, both *Podxl* and *Igfbp5* mRNAs decayed more rapidly in ES and M15 cells when *Wt*1 is deleted or downregulated respectively. To address whether WT1 is regulating gene expression through direct interactions with the 3' UTR of mRNAs, fragments with WT1 binding sites were cloned into a luciferase reporter vector. Reduced luciferase activity was observed in *Wt1* knockdown cells transfected with WT1 interacting 3' UTR fragments in comparison to the controls (**Fig. 5C**). Moreover, in a destabilized GFP reporter system, a rapid loss in GFP expression was observed in *Wt1* knockdown cells transfected with the *Igfbp5* UTR fragment that has the WT1 binding region in comparison to the control transfections which showed no change in GFP expression. (**Supplemental Fig. S5E**). We conclude that direct WT1 binding to RNA enhances the levels of mRNA targets.

In summary, we present several lines of evidence to support the conclusion that WT1 regulates the stability of mRNAs through direct interactions. In addition to the direct experimental evidence, there are other considerations that support a role for WT1 in post transcriptional regulation. Our data shows that 94% of WT1 dependent interacting target RNAs were downregulated which deviates from the published WT1 transcriptional targets. Two studies have shown that 72% (**Motamedi et al. 2014**) and 77% (**Dong et al. 2015**) of WT1 dependent transcriptional targets are downregulated, reflecting the fact that WT1 functions as a transcriptional activator or repressor. Consistent with this, only a small percentage of the downregulated WT1 interacting RNAs, overlap with the WT1 ChIPseq

targets (**Supplemental Fig. S5D**). Finally, the RNA binding motifs identified become significant on ranking based only on downregulated targets (**Supplemental Fig. S5B, S5C**). We propose that WT1 preferentially interacts with 3' UTRs and that this interaction antagonizes binding of the degradation machinery either directly or via stabilization of the mRNA structure, potentially through secondary structures (**Fig. 5D**). Although, our analysis supports a role for WT1 in stabilizing RNAs, it does not exclude a role in promoting RNA turnover.

This study has revealed a few WT1-dependent genes, *Podxl* (**Palmer et al. 2001**); *Rspo1* (**Motamedi et al. 2014**) which are both transcriptional and post transcriptional targets. Hence, for some genes, WT1 may chaperone them through various steps of the regulatory cascade. However, there is little overlap between the WT1 dependent target RNAs and WT1 transcriptional targets, emphasizing the key role of post transcriptional processes in tissue development and homeostasis. The disparity in the number of WT1 interacting RNA and WT1 regulated RNAs may imply a role for WT1 in other post transcriptional processes including mRNA localization and translation. Recent genetic evidence linking Wilms' tumor (WT) susceptibility with mutations in an exosome component (**Astuti et al. 2012**) and the microRNA processing genes (**Wegert et al. 2015**) supports the role of dysregulated RNA turnover and stability in the aetiology of WT. This resonates well with our demonstration that WT1 interacts with 3' UTR of RNA influencing stability, thus, arguing for a key regulatory role of WT1 RNA binding in the context of Wilms' Tumour.

**Materials and Methods:**

**RIP-seq:** WT1 RIP-seq on endogenous WT1 in ES and M15 cells was done by formaldehyde crosslinking followed by sonication. DNase digested samples were immunoprecipitated with WT1 antibody. Interacting RNA was purified and processed for NGS. The data obtained was analyzed using pyCRAC.

**FLASH:** UV crosslinked M15 cells were immunoprecipitated with WT1 conjugated agarose antibodies. The extracts were then treated with RNase and then formaldehyde crosslinked. The RNA protein complexes were purified after linker addition, were separated on a gel and transferred to a membrane. RNA was purified from the radioactive bands and processed for NGS analysis. Data analysis was done separately for the single reads and the hybrids obtained from FLASH.

**Transcriptome Analysis by RNA-seq:** RNA from mouse ES cell line E14, *Wt1* Knockout ES line (KO1A), M15 control, a stable lentiviral *Wt1* knockdown M15 cell line, control *lacZ*

lentiviral stable line was isolated using the Qiagen RNeasy mini columns as per manufacturer protocol. The isolated total RNA (1 μg) was Poly A selected and subjected to library preparation with the NEBnext Ultra RNA library kit for Illumina sequencing.

**qRT-PCR validation:** RNA was converted to cDNA and subjected to quantitative PCR using SyBR Green for detection. Gene expression data was analysed by ΔΔCt method. The IP data was analysed for fold enrichment. Students' unpaired t-test was used for statistical validations.

**Analysis of gene expression changes in wildtype and mutant tissues:** Crosses were set up with the *Wt1* floxed conditional with the *Wt1-GFP* knockin Nestin Cre line, E13.5 kidneys were single cell dissociated and FACS sorted using the GFP signal. RNA was isolated from FACS sorted control and mutant cells (identified by genotyping), using Trizol and followed by cDNA synthesis and qRT-PCR.

**Endogenous RNA stability assay**: Actinomycin treated control and *Wt1* knockdown cells were analyzed for gene expression at different time points.

**Luciferase Reporter Assay**: WT1 interacting 3' UTR binding fragments were analyzed for luciferase expression in a pIS1 based reporter assay in control and *Wt1* knockdown cells.

**Footnotes:** Detailed experimental procedures and data analysis is provided in Supplemental Information.

**ACKNOWLEDGEMENTS:** We thank Mrs. Anna Thornburn for help with the mouse experiments, Mrs. Rachel Middlemiss for help with lentiviral knockdowns, Dr. Elisabeth Freyer for FACS sorting, Dr. Abdel Essafi, Dr. Greg Kudla and Professor Javier Caceres for discussions and suggestions, Mr. Craig Nicol for help with graphics and MRC Core Funding to the Human Genetics Unit and MRC grant MR/N020405/1 for funding.

**REFERENCES:**

Astuti D, Morris MR, Cooper WN, Staals RHJ, Wake NC, Fews G, Gill H, Gentle D, Shuib S, Ricketts CJ, et al. 2012. Germline mutations in DIS3L2 cause the Perlman syndrome of overgrowth and Wilms tumor susceptibility. *Nat. Genet.* **44**: 277–284.

Bailey TL, Elkan C. 1994. Fitting a Mixture Model by Expectation Maximization to Discover Motifs in Bipolymers. In *Proceedings of the Second International Conference on Intelligent Systems for Molecular Biology*, **2**: 28–36.

Barbaux S, Niaudet P, Gubler MC, Grünfeld JP, Jaubert F, Kuttenn F, Fékété CN, Souleyreau-Therville N, Thibaud E, Fellous M. et al. 1997. Donor splice-site mutations in WT1 are responsible for Frasier syndrome. *Nat Genet*. **17**: 467-70.

Bardeesy N, Pelletier J. 1998. Overlapping RNA and DNA binding domains of the wt1 tumor suppressor gene product. *Nucleic Acids Res*. **26**: 1784–1792.

Bharathavikru R, Dudnakova T. 2016. Methods to Identify and Validate WT1-RNA Interaction. *Methods Mol Biol*. **1467**: 197-209.

Bor YC, Swartz J, Morrison A, Rekosh D, Ladomery M, Hammarskjöld ML. 2006. The Wilms' tumor 1 (WT1) gene (+KTS isoform) functions with a CTE to enhance translation from an unspliced RNA with a retained intron. *Genes Dev*. **20**: 1597-1608

Caricasole A, Duarte A, Larsson SH, Hastie ND, Little M, Holmes G, Todorov I, Ward A. 1996. RNA binding by the Wilms tumor suppressor zinc finger proteins. *Proc Natl Acad Sci U S A*. **93**: 7562-7566.

Chau YY, Brownstein D, Mjoseng H, Lee WC, Buza-Vidas N, Nerlov C, Jacobsen SE, Perry P, Berry R, Thornburn A, et al. 2011. Acute multiple organ failure in adult mice deleted for the developmental regulator Wt1. *PLoS Genet*. **7**: e1002404.

Chau YY, Hastie ND. 2012. The role of Wt1 in regulating mesenchyme in cancer, development, and tissue homeostasis. *Trends Genet*. **28**: 515–524.

Chau YY, Bandiera R, Serrels A, Martínez-Estrada OM, Qing W, Lee M, Slight J, Thornburn A, Berry R, McHaffie S, et al. 2014. Visceral and subcutaneous fat have different origins and evidence supports a mesothelial source. *Nat Cell Biol*. **16**: 367-375.

Davies RC, Calvio C, Bratt E, Larsson SH, Lamond AI, Hastie ND. 1998. WT1 interacts with the splicing factor U2AF65 in an isoform-dependent manner and can be incorporated into spliceosomes. *Genes Dev*. **12**: 3217–3225.

Dong L, Pietsch S, Tan Z, Perner B, Sierig R, Kruspe D, Groth M, Witzgall R, Gröne H, Platzer M, et al. 2015. Integration of Cistromic and Transcriptomic Analyses Identifies Nphs2, Mafb, and Magi2 as Wilms' Tumor 1 Target Genes in Podocyte Differentiation and Maintenance. *J. Am. Soc. Nephrol*. **26**: 2118–2128.

Essafi A, Webb A, Berry RL, Slight J, Burn SF, Spraggon L, Velecela V, Martinez-Estrada OM, Wiltshire JH, Roberts SGE, et al. 2011. A Wt1-Controlled chromatin switching mechanism underpins tissue-specific wnt4 activation and repression. *Dev. Cell* **21**: 559–574.

Hammes A, Guo JK, Lutsch G, Leheste JR, Landrock D, Ziegler U, Gubler MC, Schedl A. 2001. Two splice variants of the wilms' tumor 1 gene have distinct functions during sex determination and nephron formation. *Cell* **106**: 319–329.

Hastie ND. 2001. Life, sex, and WT1 isoforms--three amino acids can make all the difference. *Cell* **106**: 391-394.

Helwak A, Kudla G, Dudnakova T, Tollervey D. 2013. Mapping the human miRNA interactome by CLASH reveals frequent noncanonical binding. *Cell* **153**: 654–665.

Kann M, Ettou S, Jung YL, Lenz MO, Taglienti ME, Park PJ, Schermer B, Benzing T, Kreidberg JA. 2015. Genome-Wide Analysis of Wilms' Tumor 1-Controlled Gene Expression in Podocytes Reveals Key Regulatory Mechanisms. *J. Am. Soc. Nephrol.*

Kennedy D, Ramsdale T, Mattick J, Little M. 1996. An RNA recognition motif in Wilms' tumour protein (WT1) revealed by structural modelling. *Nat Genet*. **12**:329-331.

Larsson SH, Charlieu JP, Miyagawa K, Engelkamp D, Rassoulzadegan M, Ross A, Cuzin F, Heyningen V, and Hastie ND. 1995. Subnuclear localization of WT1 in splicing or transcription factor domains is regulated by alternative splicing. *Cell* **81**: 391–401.

Lu Z, Zhang QC, Lee B, Flynn RA, Smith MA, Robinson JT, Davidovich C, Gooding AR, Goodrich KJ, Mattick JS, et al. 2016 RNA Duplex Map in Living Cells Reveals Higher-Order Transcriptome Structure. *Cell* **165**: 1267-1279.

Motamedi FJ, Badro DA, Clarkson M, Lecca MR, Bradford ST, Buske FA, Saar K, Hübner N, Brändli AW, Schedl A. 2014. WT1 controls antagonistic FGF and BMP-pSMAD pathways in early renal progenitors. *Nat. Commun*. **5:** 4444.

Niksic M, Slight J, Sanford JR, Caceres JF, Hastie ND. 2004. The Wilms' tumour protein (WT1) shuttles between nucleus and cytoplasm and is present in functional polysomes. *Hum. Mol. Genet*. **13**: 463–471.

Palmer RE, Kotsianti A, Cadman B, Boyd T, Gerald W, Haber DA. 2001. WT1 regulates the expression of the major glomerular podocyte membrane protein Podocalyxin.*Curr Biol*. **11**: 1805-1809.

Sugimoto Y, Vigilante A, Darbo E, Zirra A, Militti C, D'Ambrogio A, Luscombe NM, Ule J. 2015. {hiCLIP} reveals the in vivo atlas of {mRNA} secondary structures recognized by Staufen 1. *Nature* **519**: 491–494.

Toska E, Roberts SGE. 2014. Mechanisms of transcriptional regulation by WT1 (Wilms' tumour 1). *Biochem. J*. **461**: 15–32.

Trapnell C, Roberts A, Goff L, Pertea G, Kim D, Kelley DR, Pimentel H, Salzberg SL, Rinn JL, Pachter L. 2012. Differential gene and transcript expression analysis of RNA-seq experiments with TopHat and Cufflinks. *Nat. Protoc*. **7**: 562–578.

Travis AJ, Moody J, Helwak A, Tollervey D, Kudla, G. 2014. Hyb: A bioinformatics pipeline for the analysis of CLASH (crosslinking, ligation and sequencing of hybrids) data. *Methods* **65:** 263–273.

Wagner KD, Cherfils-Vicini J, Hosen N, Hohenstein P, Gilson E, Hastie ND, Michiels JF, Wagner N. 2014. The Wilms' tumour suppressor Wt1 is a major regulator of tumour angiogenesis and progression. *Nat Commun*. **5**:5852

Webb S, Hector RD, Kudla G, Granneman S. 2014. PAR-CLIP data indicate that Nrd1-Nab3-dependent transcription termination regulates expression of hundreds of protein coding genes in yeast. *Genome Biol.* **15**: R8.

Wegert J, Ishaque N, Vardapour R, Geörg C, Gu Z, Bieg M, Ziegler B, Bausenwein S, Nourkami N, Ludwig N, et al. 2015. Mutations in the SIX1/2 pathway and the DROSHA/DGCR8 miRNA microprocessor complex underlie high-risk blastemal type Wilms tumors. *Cancer Cell* **27**:298-311.

Zhai G, Iskandar M, Barilla K, Romaniuk PJ. 2001. Characterization of RNA aptamer binding by the Wilms' tumor suppressor protein WT1. *Biochemistry* **40**: 2032–2040.

**FIGURE LEGENDS:**

**Figure 1: WT1 binds to multiple categories of RNA: (A)** Pie charts of clusters assigned to protein-coding, noncoding and other biotypes in ES (top left), M15 (bottom left) and the proportion of noncoding RNAs in ES (top right), M15 (bottom right). **(B)** The density of clusters identified by RIP-seq, ES (top), M15 (bottom), for all protein coding RNAs (blue bars), and the density at 5' and 3' ends (green and red bars respectively). **(C)** Genome Browser snapshot of alignment of RIP-seq reads from ES and M15 cell lines mapping to *Igfbp5*. **(D)** Validation of WT1 interacting protein-coding RNA biotype. *Igfbp5, Igfbp3, Pdgf, Peg3, Wnt5a, Wt1, Podxl* Interaction was confirmed by RIP in M15 cell line analyzed by qRT-PCR with target-specific primers.

**Figure 2: UV crosslinking confirms WT1 enrichment over 3' UTR of mRNAs: (A)** Schematic of FLASH protocol. **(B)** Pie charts showing the proportion of clusters of protein-coding, noncoding and other biotypes (top); noncoding RNAs (bottom) in the FLASH data. **(C)** The density of clusters identified in WT1 FLASH for protein coding (blue bars), and the density at 5' and 3' ends (green and red bars respectively). (**D**) REVIGO plot of *p* value based gene ontology terms, associated with WT1 interacting RNA, identified by FLASH.

**Figure 3: WT1 associates with RNA at the 3' UTR through secondary structures:** (**A**) Pie-charts of WT1 FLASH associated hybrids (top), compared to input (bottom) in M15 cells analyzed as energy maps. **(B)** Local hybridization in 3'UTR regions for representative targets *Igfbp5* and *Cdh11*. **(C)** RNA fold predictions of secondary structures of *Podxl* and *Wt1* 3' UTR interactions. **(D)** Heat map representation of 3' UTR intramolecular interactions in *Podxl* RNA identified by FLASH and PARIS.

**Figure 4: WT1 regulates the expression of a subset of the RNA binding targets:** (**A**) Volcano plot of transcriptome changes of E14 and *Wt1* Knockout ES cell lines (left, n=2) and the *Wt1* stable knockdown in M15 cell line compared to the *lacZ* controls (right, n=2). X-axis is $\log_2$ fold change, y-axis is $\log_{10}$ *p* value. Selected genes are highlighted. (**B**) REVIGO plot of gene ontology analysis based on *p* values of the differentially regulated genes in ES (left) and M15 (right) upon *Wt1* knockout/knockdown respectively. (**C**) WT1 interacting and regulated targets were validated by qRT-PCR. RNA changes in ES cells (Panel I); M15 cells (Panel II) compared between the knockout/knockdown and control. $\text{Log}_2$ fold changes observed in RNA-seq (n=2) and qRT-PCR (n=3) are represented in blue and red bars respectively (unpaired t test, *** $p<0.0001$, ** $p<0.001$ * $p<0.01$). (**D**) RNA changes in GFP+ FACS sorted E13.5 kidney cells compared to litter matched cre control. (n=3).

**Figure 5: WT1 regulates RNA stability: (A)** Scatterplots of log of the ratio of WT1 RIP-seq RPKM values to input (y axis) compared to the log of the ratio of coverage of genome wide (x axis); 3' UTR (grey symbols), upregulated genes (green), downregulated genes (red) (ES, top; M15, bottom). (**B**) Relative percentage expression (y axis) of genes post actinomycin treatment in hours (x axis) compared between knockout/knockdown and control cells. (**C**) Luciferase reporter activity of WT1 interacting UTR binding regions transfected in knockdown cells compared to control. Vector alone transfections represent background luciferase activity without binding regions. (**D**) A working model for WT1 RNA interaction and its functional significance.

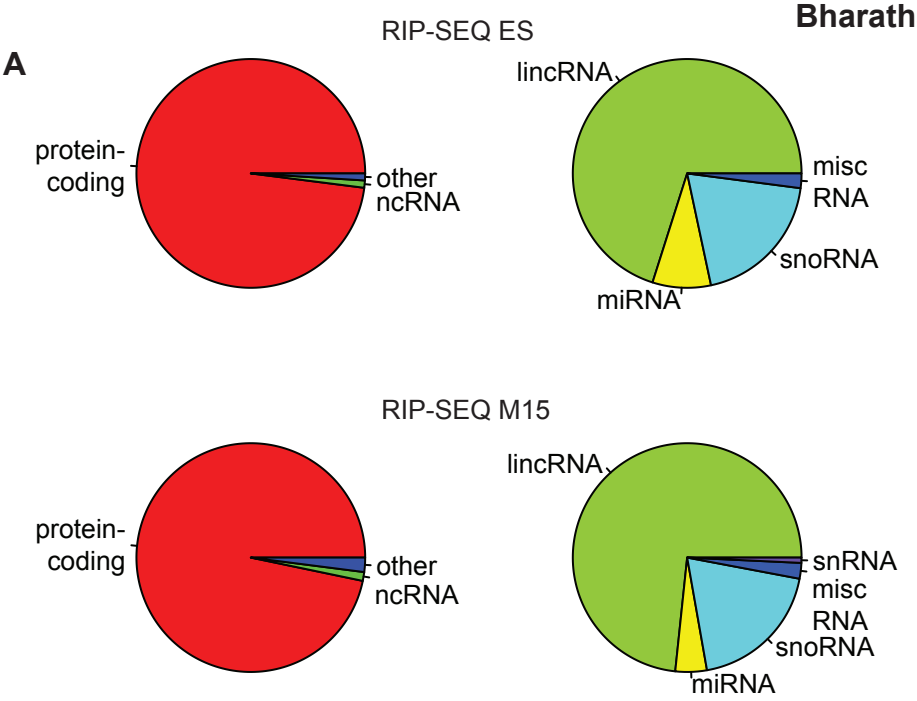
A
RIP-SEQ ES
protein-coding
other ncRNA
lincRNA
misc RNA
snoRNA
miRNA
RIP-SEQ M15
protein-coding
other ncRNA
lincRNA
snRNA
misc RNA
snoRNA
miRNA

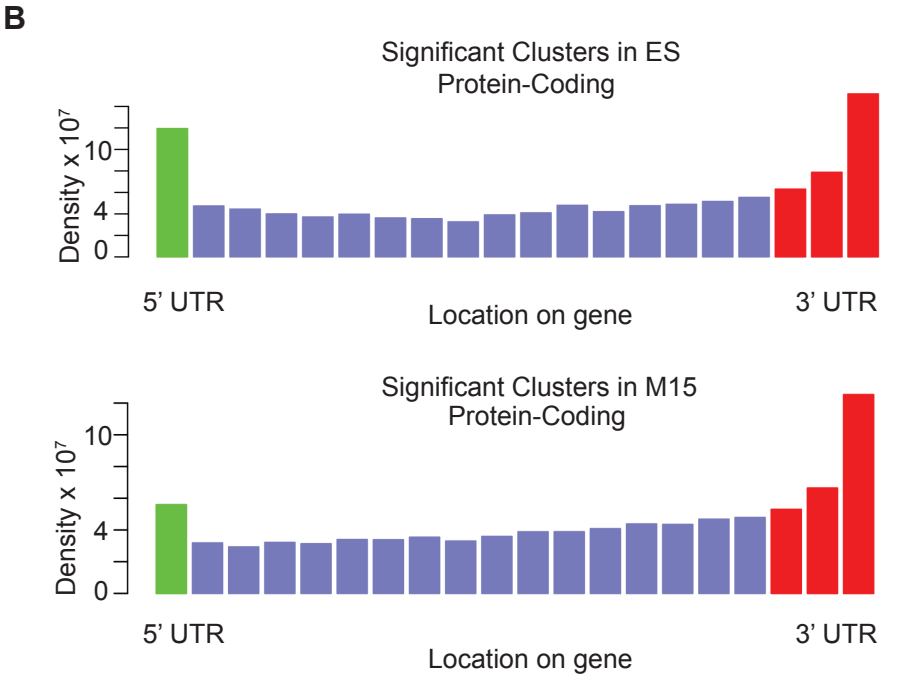
B
Significant Clusters in ES
Protein-Coding
Density x 10^7
10
4
0
5' UTR
Location on gene
3' UTR
Significant Clusters in M15
Protein-Coding
Density x 10^7
10
4
0
5' UTR
Location on gene
3' UTR

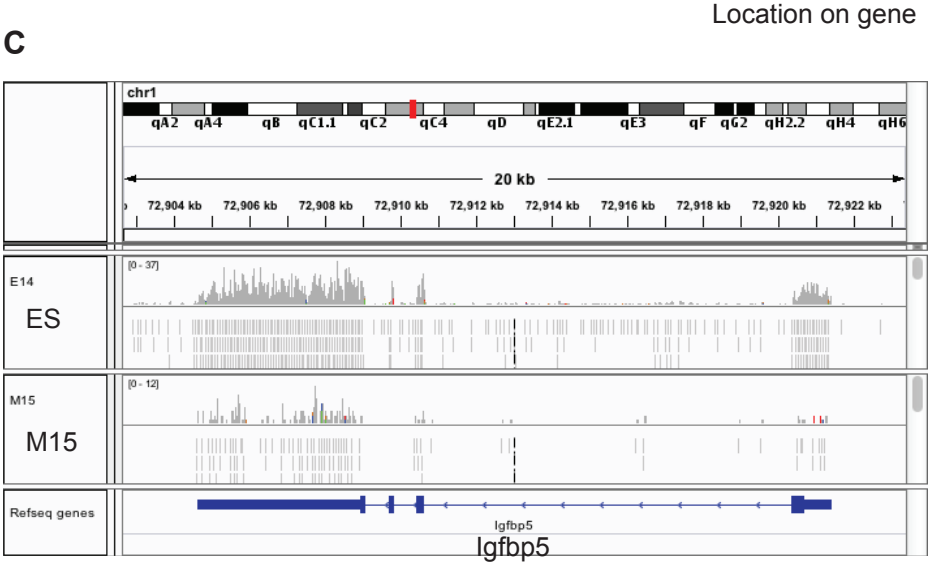
C
chr1
qA2 qA4 qB qC1.1 qC2 qC4 qD qE2.1 qE3 qF qG2 qH2.2 qH4 qH6
20 kb
72,904 kb 72,906 kb 72,908 kb 72,910 kb 72,912 kb 72,914 kb 72,916 kb 72,918 kb 72,920 kb 72,922 kb
E14
ES
M15
M15
Refseq genes
Igfbp5
Igfbp5

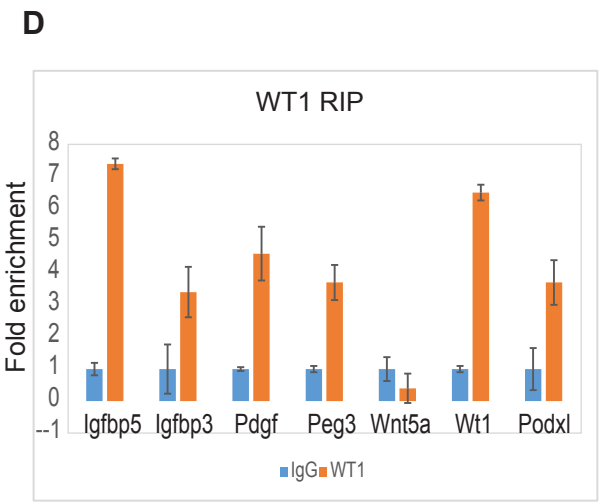
D
WT1 RIP
Fold enrichment
8
7
6
5
4
3
2
1
0
--1
Igfbp5
Igfbp3
Pdgf
Peg3
Wnt5a
Wt1
Podxl
IgG
WT1

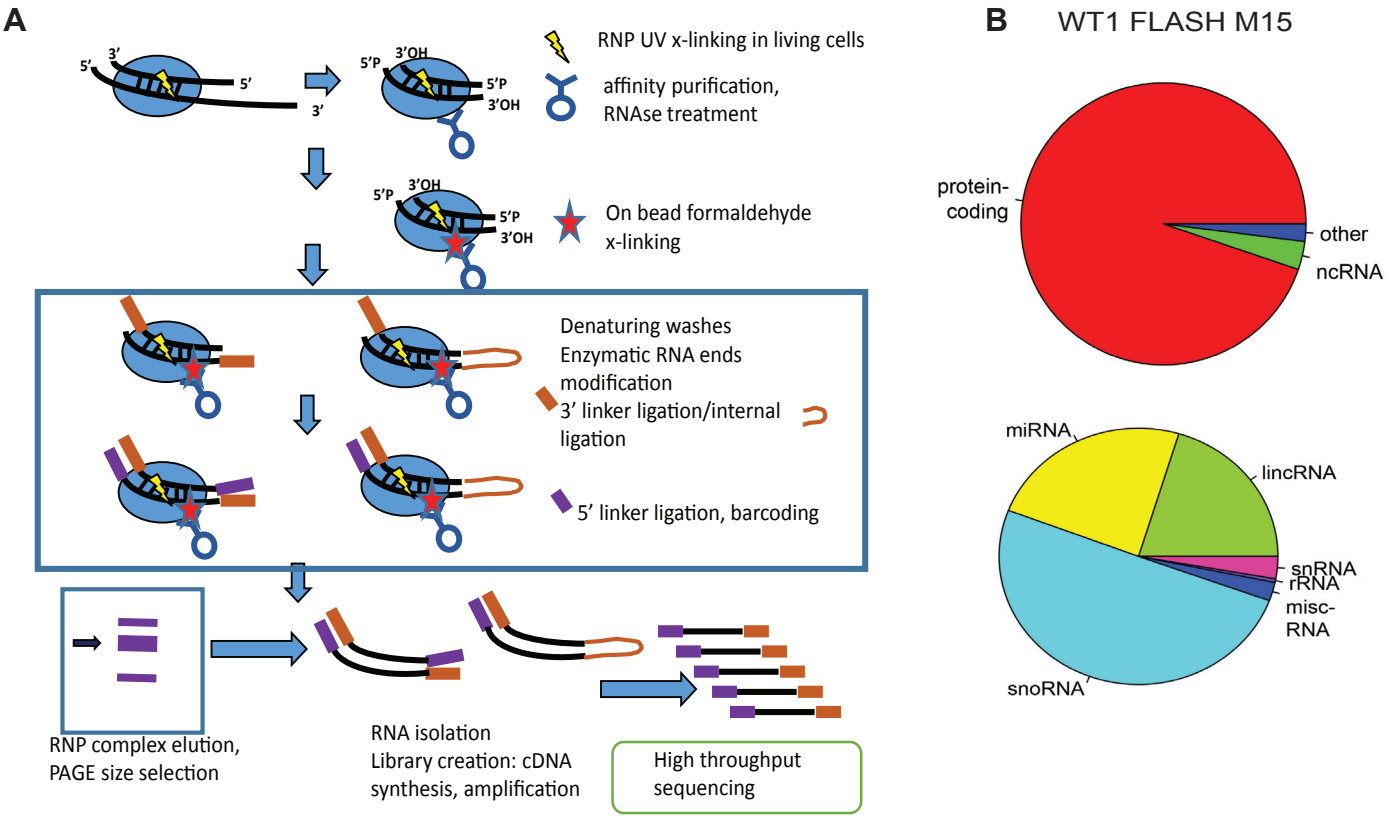
A
RNP UV x-linking in living cells
affinity purification, RNAse treatment
On bead formaldehyde x-linking
Denaturing washes
Enzymatic RNA ends modification
3' linker ligation/internal ligation
5' linker ligation, barcoding
RNP complex elution, PAGE size selection
RNA isolation
Library creation: cDNA synthesis, amplification
High throughput sequencing
B
WT1 FLASH M15
protein-coding
other
ncRNA
miRNA
lincRNA
snRNA
rRNA
misc-RNA
snoRNA

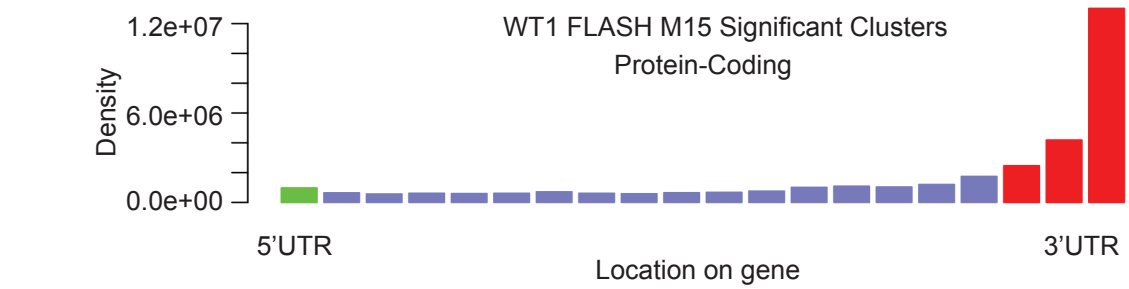
C
WT1 FLASH M15 Significant Clusters
Protein-Coding
Density
1.2e+07
6.0e+06
0.0e+00
5'UTR
3'UTR
Location on gene

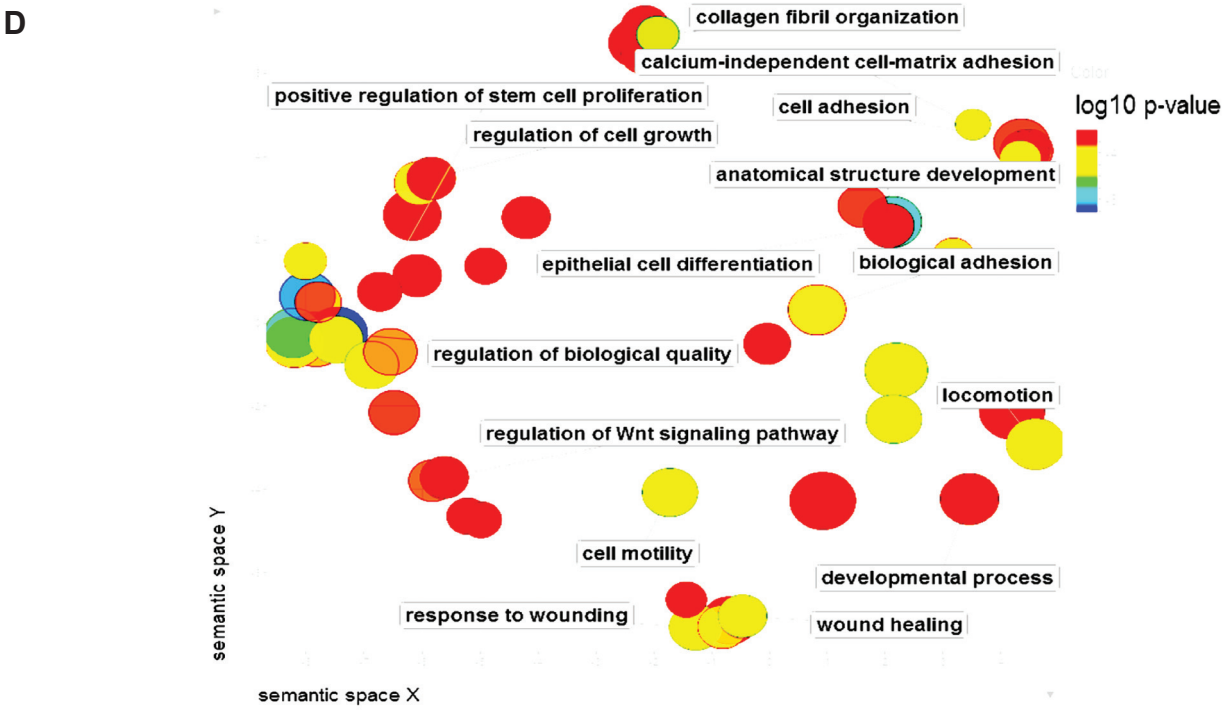
D
collagen fibril organization
calcium-independent cell-matrix adhesion
positive regulation of stem cell proliferation
cell adhesion
regulation of cell growth
anatomical structure development
epithelial cell differentiation
biological adhesion
regulation of biological quality
locomotion
regulation of Wnt signaling pathway
cell motility
developmental process
response to wounding
wound healing
log10 p-value
semantic space Y
semantic space X

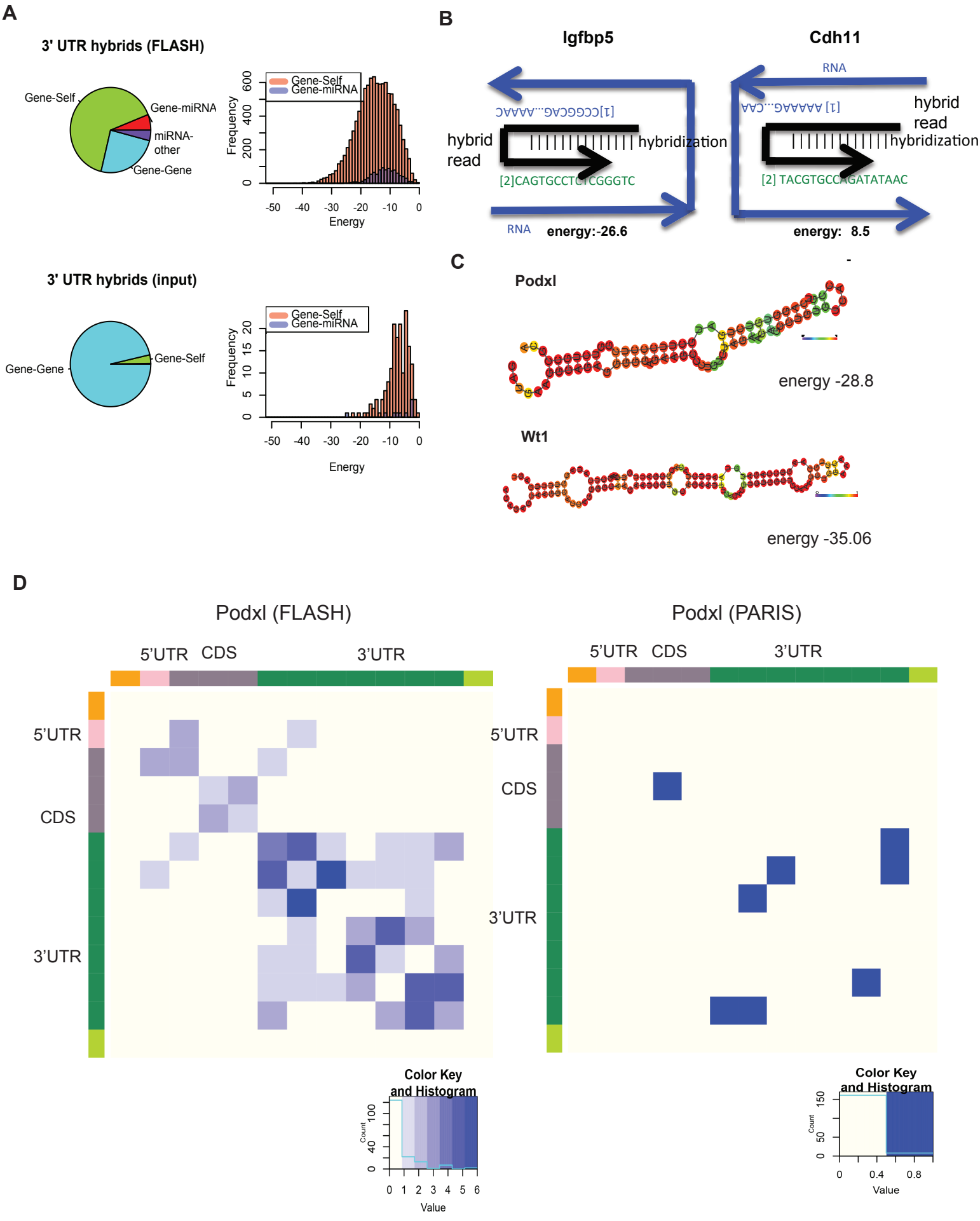
A
3' UTR hybrids (FLASH)
Gene-Self
Gene-miRNA
miRNA-other
Gene-Gene
Frequency
Energy
3' UTR hybrids (input)
B
Igfbp5
Cdh11
RNA
hybrid read
hybridization
[2]CAGTGCCTCTCGGGTC
[2] TACGTGCCAGATATAAC
energy:-26.6
energy: 8.5
C
Podxl
energy -28.8
Wt1
energy -35.06
D
Podxl (FLASH)
Podxl (PARIS)
5'UTR
CDS
3'UTR
Color Key and Histogram
Count
Value

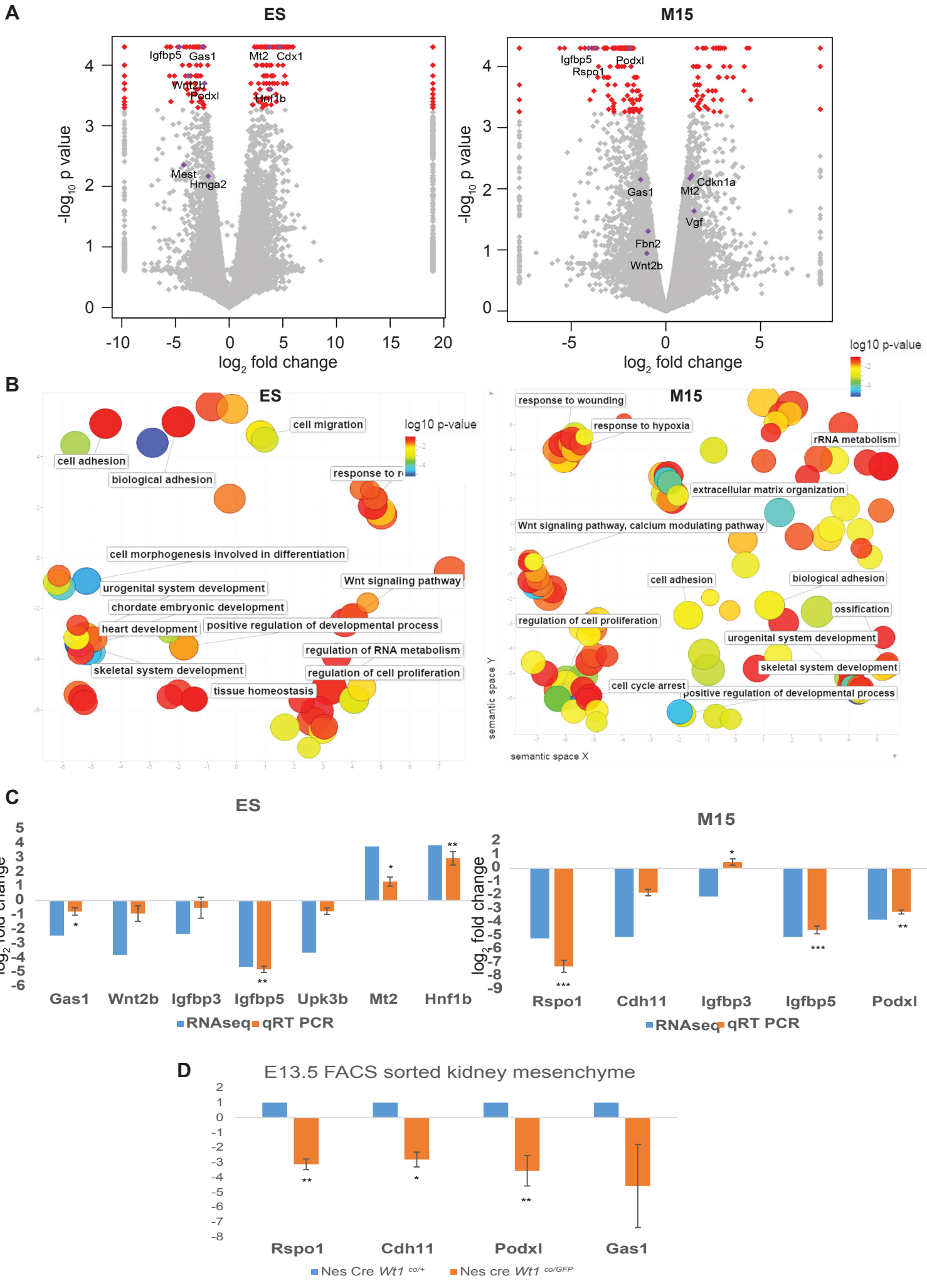
A
ES
M15
Igfbp5
Gas1
Mt2
Cdx1
Wnt2b
Podxl
Hnf1b
Mest
Hmga2
Rspo1
Cdkn1a
Vgf
Fbn2
-log10 p value
log2 fold change
B
log10 p-value
cell migration
cell adhesion
biological adhesion
response to wounding
response to hypoxia
rRNA metabolism
extracellular matrix organization
Wnt signaling pathway, calcium modulating pathway
cell morphogenesis involved in differentiation
urogenital system development
Wnt signaling pathway
chordate embryonic development
heart development
positive regulation of developmental process
regulation of RNA metabolism
skeletal system development
regulation of cell proliferation
tissue homeostasis
ossification
cell cycle arrest
semantic space X
semantic space Y
C
ES
M15
log2 fold change
Gas1
Wnt2b
Igfbp3
Igfbp5
Upk3b
Mt2
Hnf1b
Rspo1
Cdh11
Podxl
RNAseq
qRT PCR
D
E13.5 FACS sorted kidney mesenchyme
Nes Cre Wt1 co/+
Nes cre Wt1 co/GFP

Bharathavikru et al_FIGURE 5